Cooperative Counterion−Polyion Interactions in Polyelectrolyte Chain Dynamics: NMR and Quantum-Chemical Study of Locally Collapsed State in Dilute Poly(*N*-diallyldimethylammonium chloride) in NaCl/D_2O Solutions

J. Kříž,* J. Dybal, and D. Kurková

Institute of Macromolecular Chemistry, Academy of Sciences of the Czech Republic, Heyrovsky Sq. 2, 162 06 Prague 6, Czech Republic

Received: January 30, 2002; In Final Form: May 14, 2002

Using ^{1}H and ^{35}Cl single- and double-quantum NMR spectra, relaxation and pulsed gradient spin echo (PGSE) diffusion experiments combined with quantum-chemical calculations, we studied the molecular dynamics of poly(*N*-diallyldimethylammonium chloride) (PDADMAC) and its copolymers with acrylamide in D_2O under conditions of various ionic strength determined by the concentration of the polyelectrolyte itself or an added salt or both. According to absolute signal intensity, only 12−15% of the DADMAC groups are in an actual mobile state, giving rise to detectable signals. Transverse relaxation analysis shows a wide mobility distribution in the mobile groups. Double quantum ^{1}H NMR signals of *N*-methyl protons evidence motional anisotropy relative to the NMR time window and thus motional hindering in part of the visible DADMAC groups. Strong dependence of these phenomena on ionic strength, as well as quantum-chemical simulations, indicates that these phenomena are of an electrostatic nature. Probing of the counterion distribution and dynamics by ^{35}Cl NMR quadrupolar relaxation shows that a majority of counterions behave according to the Halle−Wennerström−Picullel model based on combined Poisson−Boltzmann and Smoluchowski equations, but relaxation of the $\mathbf{T_2}^3$ coherence indicates that a smaller part of the counterions correlate with the polymer motion. Accordingly, the mobile part of the polymer is interpreted as a fluctuation consisting of a locally collapsed chain and condensed counterions. By three independent methods, namely, inversion−recovery, transverse relaxation, and in particular, saturation transfer experiments, the average lifetime of this fluctuation was estimated to be in the range 30−80 ms. Thus, the fluctuation is *frozen*, that is, it is stabilized by cooperative interaction between the collapsed part of the chain and the condensed counterions. Mutual exchange between groups with different mobility, found by saturation transfer experiment, indicates that the fluctuation can move to-and-fro along the chain.

Introduction

Despite intensive research spanning 4 decades,[1−4] the structure and dynamics of polyelectrolytes has continued to attract a lively interest. This may be partly because a number of biologically important macromolecules such as nucleic acids and some proteins are polyelectrolytes and thus can be influenced by electrostatic interactions. From a more general point of view, some of the features of polyelectrolytes remain somewhat elusive. This holds in particular for their dilute solutions. Because their experimental study in a dilute regime is exceptionally difficult and prone to various artifacts of the used methods, most of the recent studies were done either in theory[5−10] or in simulation.[11−18] Neither of these approaches is quite undisputable: the polyion is frequently assumed to be a stiff rod or cylinder with symmetrically distributed charges or alternatively a flexible string of beads interacting by simple (such as Lennard-Jones) potentials; its length is taken either as infinite or, in most simulations, as quite short; the electrostatic potential is usually described in the mean-field Poisson−Boltzmann or cruder approximation, not taking the charge correlations into account; often, energy rather than Gibbs free energy (including entropy) is considered as the final criterion of the probability of a given state. Despite these limitations, which are quite understandable considering the scope and complexity of the problem, various predictions seem to converge to some important conclusions concerning polyelectrolyte molecular dynamics. In a dilute solution (the concentration of charged monomer units being on the order of 10^{-3} mol/L), the counterion space distribution strongly depends on the charge density of the polyion. For a weakly charged polyion, that is, one with the charge separation exceeding the Bjerrum length, λ_B ($\lambda_B = e^2/(\epsilon k_B T)$, ϵ being the dielectric constant, e the elementary charge, and k_B the Boltzmann constant), the counterions are distributed more or less uniformly throughout the space (although the popular Manning hypothesis apparently is not literally fulfilled), whereas for a strongly charged one, the radial counterion density increases with decreasing distance. In the latter case, a fraction of polyions is *condensed* on the polyion, that is, either intimately bound to it or distributed in its vicinity, effectively increasing its mean charge distance approximately to λ_B. Considering now the polyion itself, electrostatic repulsive interaction between the like charges forces its backbone into a more extended conformation, thus increasing its electrostatic persistence legth[19] (due to short-range interactions), as well as end-to-end distance (due to long-range interactions) of the chain. Expectedly, this effect is weakened by counterion condensation, as well as salt additions to the solution. According to simulations, the added electrolyte does

* To whom correspondence should be addressed. kriz@imc.cas.cz.

10.1021/jp020282k CCC: $22.00
Published on Web 08/07/2002

SCHEME 1

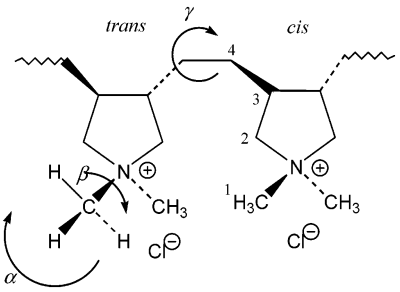

not increase substantially the fraction of condensed counterions but has a screening effect on the electrostatic repulsions. Partial chain collapse (i.e., less extended or more coillike conformation with shortened end-to-end distance and shortened electrostatic persistence length) of flexible, as well as stiff, polyions thus has been predicted to be an effect of salt addition[8,14,15] or, in the case of stiff polyelectrolytes, of counterion density fluctuations.[9] It can be expected that the interactions (repulsions, charge neutralization, screening) affecting the electrostatic persistence length should have an analogous effect on the chain dynamics of the polyion, that is, on the extent and frequency of its conformation changes. Counterion condensation and ion screening thus should make the polyion chain more flexible in the dynamic sense, too.

Considering the limitations of available theoretical or simulation methods, experimental results in this field would be welcomed. Apart from individual studies of special effects in biological macromolecules, systematic data appear to be meager, however. Dynamic light-scattering (DLS) studies, after clarification of specific effects,[20−22] find the electrostatic persistence length of flexible highly charged polyelectrolytes at vanishing concentration to be scaled by the Debye screening length, $1/\kappa$ ($\kappa^2 = \lambda_B \sum c_i z_i^2$, the sum being equal to the ionic strength). Unfortunately, the potentially very useful complementary NMR studies were mostly precluded by insufficient concentration sensitivity. However, self-diffusion of a polyanion, measured by a pulsed-field-gradient NMR, shows a behavior corresponding to a rod, in fair agreement with DLS data.[23] Only qualitative data of the chain dynamics from ^{1}H NMR of a dilute polyion appear to be at hand.[24] As for the counterion distribution, both NMR relaxation[24−27] (quadrupolar nuclei) and self-diffusion[28] studies point to some condensation in dilute solutions.

NMR generally is a very efficient tool for the study of local and semilocal dynamics of polymers. The difficulty in using it as a probe into the dynamics of dilute polyelectrolytes lies in the sensitivity of the method. The signals of skeletal protons (not mentioning other nuclei) are usually broadened and very weak so that most available methods of study are impracticable. However, there is one type of polyelectrolyte,[29] namely, poly(*N*-diallyldimethylammonium chloride) (PDADMAC) containing two methyl groups attached to the polymer backbone in a way that makes their signals usually measurable and, at the same time, very sensitive to the mobility of a DADMAC group.[30] Broadening or apparent extinction (i.e., extreme broadening) of these signals, analogous to that of $N-CH_3$ signals in another type of polycation,[31] has been observed as a result of a relative immobilization of the DADMAC group due to its coupling to a polyanion. In the present study, we use the same phenomenon as a probe into the dynamics of PDADMAC itself.

As a semiflexible (rigid five-membered rings interleaved by flexible CH_2-CH_2 bonds, see Scheme 1) and medium-charged (charge separation being almost exactly that of λ_B at 25 °C) polyelectrolyte, PDADMAC stands in the middle between the extremes usually dealt with in theory. This makes it a particularly interesting object of study.

Experimental Section

Materials Used. DADMAC polymer and its copolymers with acrylamide were prepared[29] by radical polymerization of the DADMAC monomer. Their solutions in 99.9% D_2O (Aldrich) were prepared by simple dissolution of the polymer. The corresponding solutions in NaCl/D_2O were prepared by slow mixing of more concentrated solutions (20 mmol DADMAC/L, 0.1 mol NaCl/L) and subsequent dilution of the mixtures by D_2O. Unless differently stated, the final solutions contained 2 mmol/L DADMAC groups.

NMR Measurements. ^{1}H and ^{35}Cl NMR spectra, relaxations, and pulsed-field-gradient stimulated spin−echo (PFG-SSE) measurements were measured using a Bruker Avance DPX300 instrument with a broadband inverse-detection probe head (proton spectra, relaxations, and PFG-SSE) or broadband direct-detection probe head (^{35}Cl spectra and relaxations). Most of the methods used were described earlier.[30,31] ^{1}H single-quantum spectra were measured using WATERGATE suppression or digital filtering of the residual HOD signal. ^{1}H double-quantum[32,33] and ^{35}Cl double-quantum[35−37] $\mathbf{T_2}^3$ spectra and relaxations were measured using the standard $d_1-\pi/2-d_2-\pi-d_2-\pi/2-d_3-\pi/2-$FID sequence, d_2 being 50 μs and d_3 incremented in the relaxation measurements. To avoid phase distortions, all ^{35}Cl NMR spectra were measured in a spin−echo mode. Longitudinal relaxations thus were measured using a modification of the conventional inversion−recovery experiment, namely, $d_1-\pi-vd-\pi/2-d_2-\pi-d_2-$FID ($d_2 = 50$ μs), transverse relaxations using the simple $d_1-\pi/2-vd-\pi-vd-$FID sequence with vd incremented. At least 180 000 scans (3.5 h) were collected in one experimental point (2.3 days for a typical 16 point experiment). ^{1}H PFG-SSE measurements were done using the simple Tanner sequence with 3 ms pulses of field gradients incremented in the range 15−50 G/cm and constant diffusion delay (typically 30 ms for ^{1}H, 3 ms for ^{35}Cl).

Results and Discussions

^{1}H NMR Single Quantum Coherence (SQC) and Double Quantum Coherence (DQC) Spectra, Relaxations and PFG-SSE Measurements of PDADMAC at Varying Ionic Strength. The dilute regime of polyelectrolytes is often believed to start at concentrations below 0.01 mol/L of the charged groups. In the case of strongly charged polyelectrolytes, however, characteristic effects of this regime emerge at 2 mmol/L and below. Therefore, we have chosen the concentration of 2 mmol/L of DADMAC groups for this study, although it is extremely low from the point of view of NMR (it corresponds to about 0.03% w/w, that is, more than 2 orders of magnitude below the usual concentration). The low concentration, combined with the width of the signals, makes the study technically challenging. Measurement of any kind of nuclei except ^{1}H and ^{35}Cl are excluded on sensitivity reasons and so are some ^{1}H techniques such as high-resolution MAS and most 2D techniques. Each of the spectra (or points in relaxation or PFG measurements) was obtained collecting at least 800 scans (corresponding to 1 h, at least, of measurement) using a very sensitive inverse-detection probe.

Figure 1 compares ^{1}H NMR spectra of PDADMAC in pure D_2O and solutions with increasing NaCl concentration. The assignment of signals corresponds to Scheme 1; suffixes a and

Figure 1. ^{1}H NMR spectra of PDADMAC (2 mmol/L) at 0, 2, 5, 10, 20, and 40 mmol NaCl/L (from bottom, absolute intensities adjusted) in D_2O (300 K).

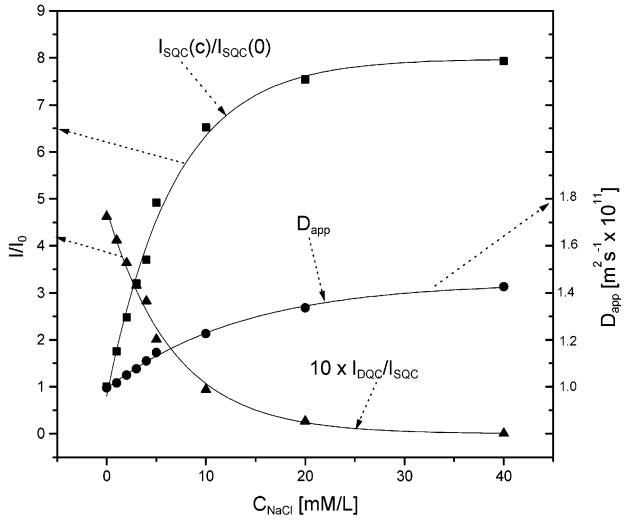

Figure 2. Absolute intensities of single quantum signals (normalized to the intensity at $C_{NaCl} = 0$), relative intensities of double-quantum signals and apparent self-diffusion coefficients (from PGSE) of PDADMAC ($M_n = 1.6 \times 10^5$, $C_{DADMAC} = 2$ mM/L) in dependence on NaCl concentration (D_2O, 300 K).

b mean nonequivalent protons or groups, and c and t mean DADMAC groups bonded in cis or trans configuration in the polymer. It is apparent that increasing ionic strength of the medium makes all signals narrower and more intensive. The intensity change for PDADMAC with $M_w = 4.35 \times 10^5$ is shown in Figure 2, in which the absolute intensity of the group of *N*-methyl signals increases up to almost 8 times the lowest

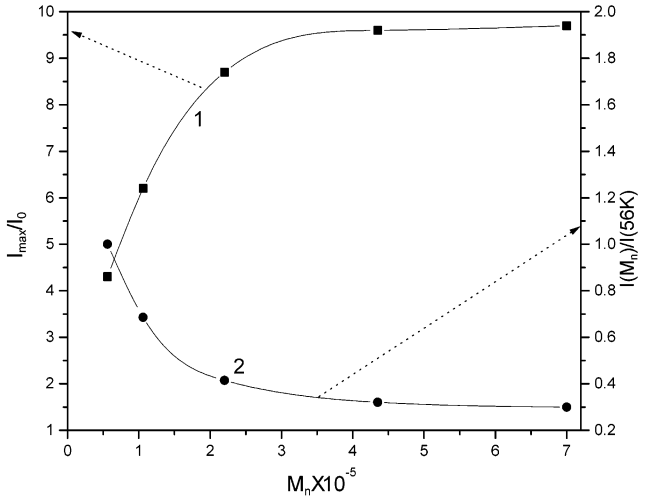

Figure 3. Molecular weight dependence of intensities of signals 1 at 20 mmol/L NaCl relative to those in pure D_2O (line 1) and of absolute intensities normalized to that of $M_w = 5.6 \times 10^4$ (line 2) at 300 K.

value in the interval 0−40 mmol NaCl/L. An analogous change can be observed for all signals of the spectrum, only with less certain quantification due to larger widths of the signals. The intensity increase due to added salt decreases with increasing PDADMAC concentration (being thus clearly caused by ion shielding due to the increased ionic strength). It also depends on the molecular weight of PDADMAC as shown in Figure 3, but the dependence is convergent above $M_n \approx 3 \times 10^5$. The effect is thus connected with a fully developed polyelectrolyte nature of the polymer rather than with the ends of the chain. It is highly reproducible and corresponds to experimental conditions ensuring the usual additivity of NMR signals. Because the concentration of DADMAC groups is constant in all samples, the only plausible explanation of the phenomenon is extreme broadening of some components of the signals (i.e., signals of some of chemically analogous groups) due to residual static dipolar interactions. Such broadening, though less extreme, also affects some components of the visible signals, in particular, at low ionic strength. This is clearly demonstrated by the course of single-quantum coherence (or transverse) relaxation discussed below.

Extreme signal broadening in proton NMR is mostly caused by residual static dipolar interactions due to impaired local mobility of the molecule. This cause is verified by the existence of double-quantum coherence *N*-methyl signals, which can be detected with a relative intensity decreasing with higher ionic strength (see Figure 2). In low-molecular-weight compounds and most polymers in solution, protons in an isolated methyl group cannot give rise to a dipolar order (and thus to multiple quantum signals) because their spin state is degenerate due to a very fast rotation. This holds for an effectively isotropic motion, however. As demonstrated by several authors,[32,33,39] even anisotropy relative to a characteristic time window can offer conditions for a multiple-quantum coherence signal. In our case (cf. Scheme 1), even very fast rotation, α, and wobbling of the axis, β, cannot provide for truly isotropic motion if the skeletal rotation, γ, is hindered. As apparent in Figure 2, the fraction of "visible" groups with such a type of motion decreases with increasing ionic strength. This indicates a changing distribution of local mobility of these groups under changing conditions.

The existence of a rather broad mobility distribution, in particular, at low ionic strength, is clearly demonstrated by the course of transverse relaxation of the single-quantum coherence

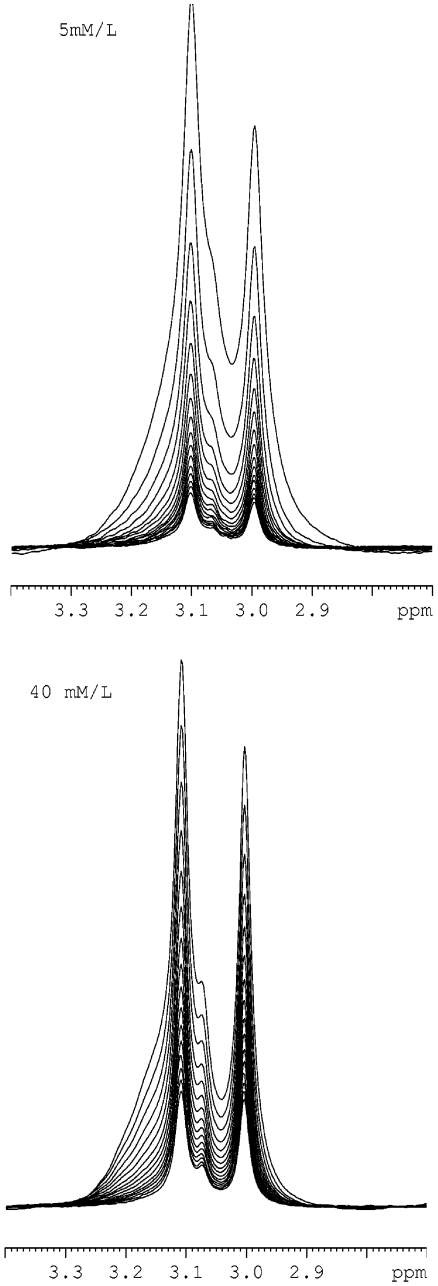

Figure 4. N−CH_3 region in ^{1}H NMR spectra of PDADMAC (2mM/L in D_2O) in the presence of NaCl (5.0 and 40.0 mM/L) after 4, 12, ..., 124 ms transverse relaxation.

signals. In all cases, the decay curves are distinctly polyexponential. Accordingly, the signals become narrower in the course of relaxation, because their broader components decay faster. This is illustrated by two examples in Figure 4: the signals originally much broader and faster decaying at lower NaCl concentration (5 mmol/L) decay to virtually the same shape (though lower relative intensity) as do those at higher salt content (40 mmol/L). Therefore, we analyzed the time change of both intensity and shape of the signal 1bc for each relaxation assuming the signal to be a superposition of a finite number of Lorentzian curves, according to eq 1,

$$I_\nu(t) = \sum_i A_i \exp(-t/T_{2i}) \frac{T_{2i}}{4\pi^2(\nu - \nu_0)^2 T_{2i}^2 + 1} \qquad (1)$$

Equation 1 is a rather crude approximation, because the broader

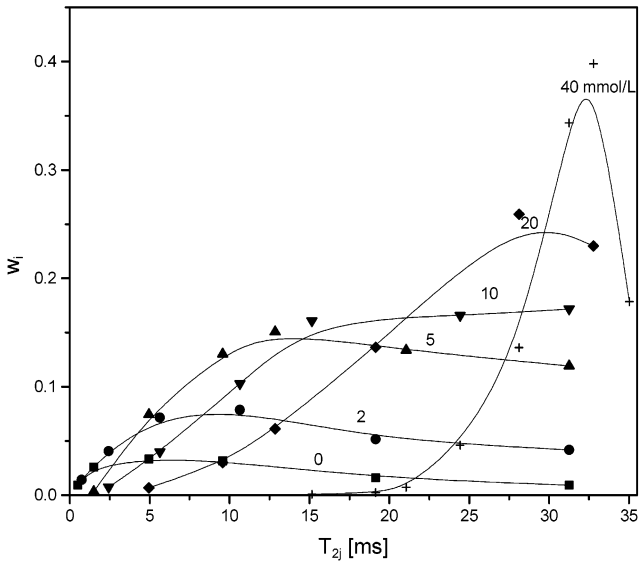

Figure 5. Reconstructed distributions (w_i are A_i in eq 1 normalized so that $\sum w_i = 1$ at full signal intensity) of transverse relaxation times in the visible parts of N−CH_3 ^{1}H NMR signals (1cb) of PDADMAC at NaCl concentrations 0, 2, 5, 10, 20, and 40 mmol/L in D_2O (DADMAC concentration 2 mmol/L, 300 K).

components can be expected to have, at least partially, Gaussian shape and the whole superposition could be somewhat distorted by mutual exchange. Because the least-squares fitting algorithm cannot effectively handle more than five or six components and a substantial part of the signal is not visible, there is not enough information for an exact analysis. We thus present in Figure 5 the distributions obtained by fitting only as a semiquantitative illustration of the following tendency. At all levels of ionic strength, the signal contains a component with $\Delta\nu_{1/2} = 9-10$ Hz (corresponding to $T_{2i} = 32-35$ ms), that is, broadened almost solely by interaction with the quadrupolar ^{14}N. This component probably corresponds to almost free skeletal rotation γ, and its intensity is both absolutely and relatively highest at 40 mmol NaCl/L. At lower salt concentration, as the signal progressively "drowns" in noise, broader signal components increase in relative intensity and the relative maximum of the visible distribution is shifted toward $\Delta\nu_{1/2} = 42.4$ Hz ($T_{2i} =$ 7.5 ms, by interpolation for 2.0 mmol/L NaCl) and more.

The most plausible way of interpreting these results is the following. At zero salt concentration, there is a small fraction (about 2%) of DADMAC groups that are motionally almost free, surrounded by progressively less mobile groups (up to about 10% at $M_n > 2 \times 10^5$) and, farther along the chain, by a majority of motionally hindered parts of the chain. The relative hindrances are progressively removed by increasing ionic strength so that, at $C_{NaCl} > 30$ mmol/L, the mobility of the whole chain is almost uniform and full. Because the motional hindrances are removed by ion screening, they must be of an electrostatic nature. They are the well-known long-range repulsions, which increase the electrostatic persistence length and extend the chain conformation in polyelectrolytes. Such interactions can be weakened by ion screening, as is observed in our case. This is also verified by the increase in the apparent self-diffusion coefficient (decrease in hydrodynamic radius) with increasing ionic strength in Figure 2. Analogous increase in D_{app} with increasing ionic strength and concentration was observed for polyions both by pulsed gradient spin echo (PGSE)[28] and DLS.[20]

As shown below by quantum-mechanical simulations, the locally more mobile state of the polyelectrolyte corresponds to

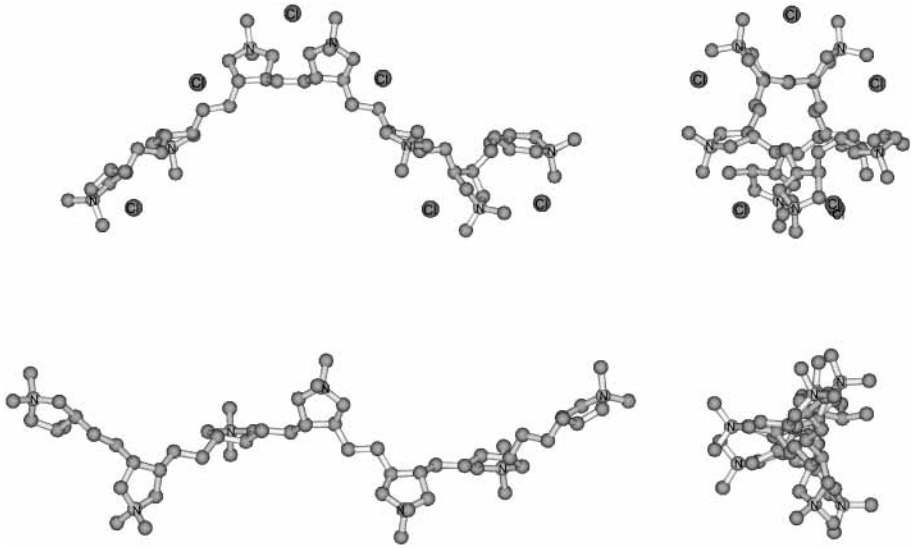

Figure 6. Two projections of the optimum molecular shapes of the DADMAC heptamer in the ion-pair (above) and bare polycation (below) forms as obtained by MNDO simulation. The chains form 5/1 and 3/1 helices with the radius 0.50 and 0.36 nm and the charge distance projected on the axis of the helix 0.43 and 0.49 nm, respectively.

(i) larger screening of the repulsive Coulomb interactions of its positive charges, that is, stronger counterion condensation and (ii) to a locally collapsed, that is, less extended chain. Such a perturbation can arise by a local counterion density fluctuation, as predicted[9] by Golestanian, Kardar, and Liverpool for rigid polyelectrolytes. In a semiflexible polyelectrolyte such as PDADMAC, it can survive long enough to be observed by NMR only due to a cooperative counterion−polycation interaction.

Quantum-Mechanical Simulations of the Preferred Chain Conformation and Rotational Hindering. To confront our interpretation of the above results with theoretical predictions, we optimized the structure of a DADMAC oligomer. Figure 6 shows two projections of the optimum molecular shapes of the DADMAC heptamer in the ion-pair and bare polycation forms, as obtained by MNDO simulation. The chains form 5/1 and 3/1 helices, with the radius 0.50 and 0.36 nm and the charge distance projected on the axis of the helix 0.43 and 0.49 nm, respectively. In agreement with many published MD and electrostatic simulations made on other polyelectrolytes, the chain is thus predicted to be substantially more extended in its ionized form. It can be expected that the barrier to the γ rotation (cf. Scheme 1) should also depend on the ionization state of the charged groups of the polyelectrolyte. To get a quantitative estimation of this effect, we simulated the energy profile of the γ rotation of a DADMAC dimer both in its bare dication and contact ion pair state. The results obtained by the MNDO method are shown in Figure 7. The differences of the shape and height of these profiles is striking. The respective rotation barriers are 9.61 and 6.28 kcal/mol according to MNDO. Because the precision of a semiempirical method is not always trustful, we repeated the calculations for both rotational extremes using an ab initio SCF/DFT quantum-mechanical method (B3LYP/6-31G(d)), obtaining barriers of 11.09 and 6.95 kcal/mol, respectively. Considering the difference, 4.14 kcal/mol, we could expect about a 10^3 times faster rotation in the electrically neutral (or effectively screened) state. This estimation forms an upper bound to the real case, because the calculations correspond to the vacuum state. Nonetheless, these results strengthen the argument that the electrostatic hindering of skeletal conformational changes, giving rise to dipolar broadening of the $N-CH_3$ NMR signals, can be effectively removed by counterion condensation or ion screening.

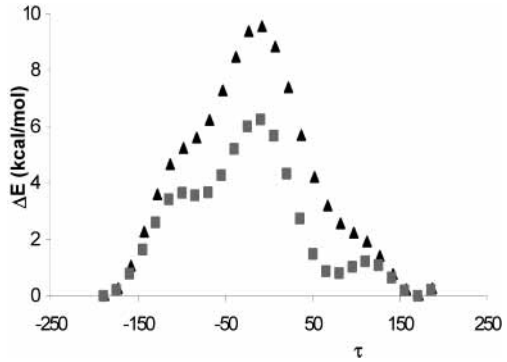

Figure 7. Dependences of the relative energy of the DADMAC dimer ((▲) bare dication, (■) form containing two Cl^- ions in contact pairs) on the torsion angle τ according to MNDO. The respective rotation barriers for the first and second form are 9.61 and 6.28 kcal/mol (MNDO) and 11.09 and 6.95 kcal/mol (B3LYP/6-31G(d)).

Viewed in the most common approximation as a charged cylinder, PDADMAC should be considered to be strongly charged (the charge distance projected on the cylinder axis being 0.491 or 0.435 nm, respectively), although the predicted actual distance of the charged nitrogen atoms is 0.870 and 0.723 nm, respectively, exceeding thus the value of the Bjerrum length ($\lambda_B = 0.698$ nm in H_2O at 300 K). In the ion pair form, the counterions sit in intermediary positions between two neighboring cations. In an aqueous solution, they can be expected to move around in hydrated forms. According to our calculations, the first hydration shell of a lone counterion has no ion-related structure; rather, the ion makes a hole in a natural configuration of water. Such configuration is easily deformed by encounter of the ion with another charged species. Figure 8 compares the optimized geometries predicted by an ab initio/DFT calculation for contact pairs of a DADMAC model in the bare and hydrated states. As shown, N−Cl distance is increased by more than 0.1 nm in the hydrated state but the symmetry of the first hydration shell is grossly distorted. Analogous but less-pronounced distortion can be predicted at further distances from the polyion.

Probing the Counterion Behavior by ^{35}Cl Quadrupolar Relaxation. According to the above shown results, counterion

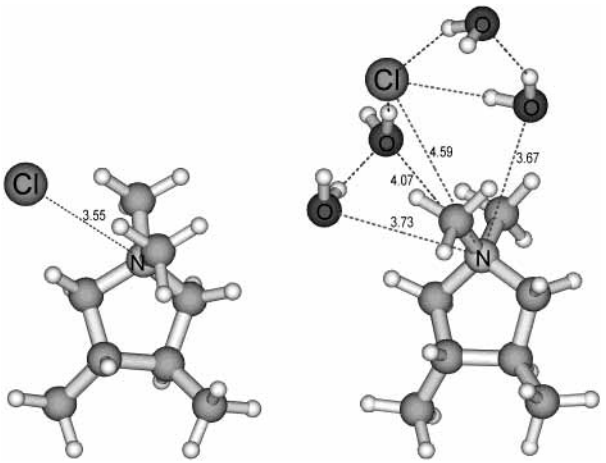

Figure 8. Optimized geometries of contact ion pairs of a DADMAC model with bare (left) and hydrated (right) chloride counterions (B3LYP/6-31G(d)).

distribution is crucial for the local and semilocal mobility of the polycation. To some degree, it can be studied using quadrupolar relaxation of the ^{35}Cl nuclei although it is somewhat difficult because of relatively low receptivity and fast relaxation of ^{35}Cl in bound ions.

Relaxation of ^{35}Cl in chloride counterions of PDADMAC is much faster than expected, considering its nuclear quadrupolar moment (about 0.66 in absolute value of that of ^{23}Na). Its peculiarity was already detected and interpreted by Hertz and Holz.[35] According to their findings, fast relaxation in "structure breaking" ions is caused by an easy deformation of their hydration shell during encounter with another charged species, in particular, that containing organic parts to which the water molecules are transiently bound by hydrophobic hydration. Because the only other charged species in PDADMAC solutions are the polycation chains, this phenomenon should only make ^{35}Cl quadrupolar relaxation more sensitive to the distribution of the chloride ions relative to the chain.

Our analysis is mostly based on the model of quadrupolar transverse relaxation of $I = {}^3/_2$ nuclei in polyelectrolyte counterions given by Halle and co-workers[26,27] The authors treat the polyion as a rigid cylinder with a radius a in a cylindrical cell with a radius $b = (\pi l n_m)^{-1/2}$, l and n_m being the monomer length and number density, respectively. The most important factor in transverse relaxation of the counterion nuclei ($I = {}^3/_2$) is shown to be diffusion of the counterions across the cell's boundary from one polyion to another (differently oriented) one. In dilute solutions of densely charged polyions, the correlation function of the residual electric field gradient (efg) of the polyion has a long-time tail, and consequently, the relaxation behavior becomes dominated by the zero-frequency spectral density, $J(0)$. In first approximation, $J(0)$ is shown to depend on the probability P of the counterion being present in the perturbed area $r \in \langle a, a + \delta \rangle$, where δ is supposed to be on the order of the first hydration shell radius of the counterion, and on the rate of its diffusion out of the cell, given by the inverse of the radial correlation time, τ_{rad}. The average density distribution of the counterions is based on the mean-field Poisson−Boltzmann equation

$$-\epsilon_0\epsilon_r \frac{1}{r}\frac{\mathrm{d}}{\mathrm{d}r}\left[r\frac{\mathrm{d}\psi(r)}{\mathrm{d}r}\right] = \sum_i z_i e n_i(b) \exp\left[-\frac{z_i e \psi(r)}{k_B T}\right] \quad (2)$$

Their translational diffusion is treated accordingly, using the

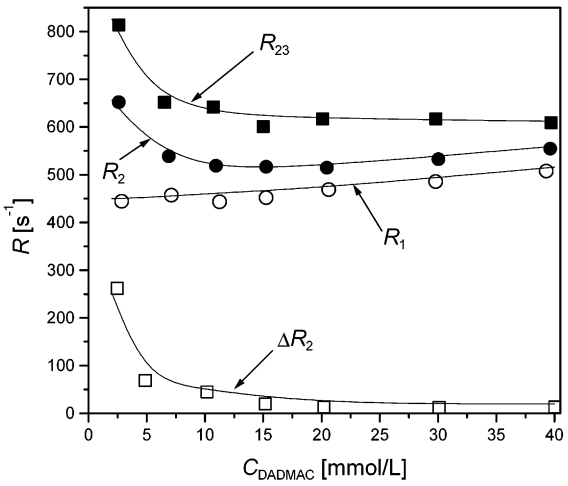

Figure 9. Experimental ^{35}Cl R_1 (longitudinal), R_2 (transverse), calculated ΔR_2, and measured R_{23} ($\mathbf{T_2}^3$) relaxation rates at various DADMAC concentrations.

Smoluchowski equation

$$\frac{1}{D}\frac{\partial}{\partial t}f(r,t) = \frac{1}{r}\frac{\partial}{\partial r}\left[\frac{\partial}{\partial r} + \sum_i \frac{z_i e}{k_B T}\frac{\mathrm{d}\psi(r)}{\mathrm{d}r}\right] f(r,t) \quad (3)$$

where $\psi(r)$ and $f(r,t)$ are the electrostatic potential at r and probability to find a counterion in the interval from r to $r + \mathrm{d}r$, respectively. With eqs 2 and 3 solved for the given system, both P and τ_{rad} are obtained. The model defines a relaxation rate difference, ΔR_2,

$$\Delta R_2 \equiv R_2^+ - R_2^- = (2\pi^2/3)[J(0) - J(2\omega_0)] \quad (4)$$

where $J(0)$ and $J(2\omega_0)$ are the spectral densities at zero and double Larmor frequency, respectively. According to the model, ΔR_2 can be approximated as follows:

$$\Delta R_2 = (\pi^2/20)\overline{\chi_Q}^2 P^2 \tau_{rad}/(1 - S_2) \quad (5)$$

where $\overline{\chi_Q}$ is an effective quadrupolar splitting constant at δ and S_2 is an order parameter (supposed to be zero in dilute solutions). ΔR_2 can be obtained from a careful analysis of the biexponential decays in transverse (or $\mathbf{T_1}^1$)

$$\langle I_x(t)\rangle + i\langle I_y(t)\rangle = [\langle I_x(0)\rangle + i\langle I_y(0)\rangle]\, \mathrm{e}^{-i\omega t}\left\{\frac{3}{5}\exp(-[J(0) + J(\omega_0)]t) + \frac{4}{5}\exp(-[J(\omega_0) + J(2\omega_0)]t)\right\} \quad (6)$$

and longitudinal (or $\mathbf{T_0}^1$) relaxation[36]

$$\langle I_z(t)\rangle = \langle I_z(0)\rangle\left\{\frac{1}{5}\exp[-J(\omega_0)t] + \frac{4}{5}\exp[-J(2\omega_0)t]\right\} \quad (7)$$

In the case of ^{35}Cl counterions and at concentrations below 10 mmol/L, such analysis is rather involved because of low effective sensitivity of the measurement (2- to 6-day experiments have to be performed for each decay).

Figure 9 shows concentration dependences of ^{35}Cl R_1 (longitudinal, $\mathbf{T_0}^1$) and R_2 (transverse, $\mathbf{T_1}^1$) relaxation rates obtained by monoexponential fitting of the experimental decays. As expected by the Halle−Wennerstrom−Picullel model,[26,27] the difference between them markedly increases at low concentrations. The values of ΔR_2, obtained by careful biexponential fitting, are also shown in Figure 10. The marked increase of

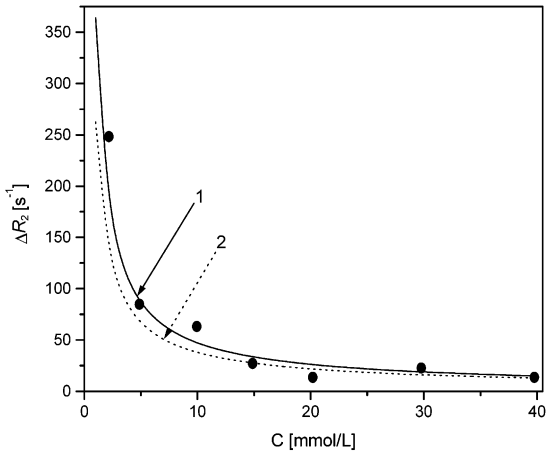

Figure 10. Experimental ^{35}Cl $\mathbf{T_2^3}$ relaxation rates, ΔR_2 (points), at various DADMAC concentrations and simulated $\Delta R_2(c)$ dependences for (1) condensed counterions ($a = 0.504$, $l = 0.435$ nm) and (2) dissociated ($a = 0.365$, $l = 0.491$ nm) ions ($\chi_Q = 153$ kHz, $D = 2.032 \times 10^{-9}$ m^2 s^{-1}, $T = 300$ K).

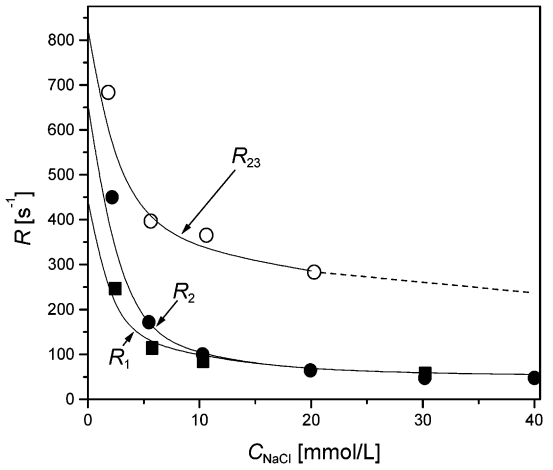

Figure 11. Dependences of the longitudinal (R_1), transverse (R_2), and double-quantum (R_{23}) relaxation rates of ^{35}Cl ions in PDADMAC−NaCl solutions on NaCl concentration (D_2O, 300 K).

this value can again be seen at low concentrations. Figure 11 shows fitting of these values using eqs 2, 3, and 5 for two types of geometries obtained by quantum mechanical calculations and reported above: (1) condensed counterions ($a = 0.504$, $l = 0.435$ nm, cf. Scheme 2) and (2) dissociated ($a = 0.365$, $l = 0.491$ nm) ions. The calculations were done using $\chi_Q = 153$ kHz, $\delta = 7$ nm, $D = 2.032 \times 10^{-9}$ m^2 s^{-1}, and $T = 300$ K. The value of χ_Q is larger than that used by Halle and co-workers[26,27] for ^{23}Na (71 kHz). We think this value to be reasonable, although the quadrupole moment of ^{35}Cl is (in absolute value) about 0.66 of that of ^{23}Na. As already shown by Hertz and Holz,[41] the markedly faster relaxation of ^{35}Cl (and analogous *structure breaking* ions) is due to much easier deformability of their solvation spheres, in particular, due to hydrophobic hydration of the organic part of the complementary ion. The latter phenomenon is also predicted by our quantum mechanical calculation reported above. As shown in Figure 10, the model fits somewhat better to the geometry predicted by our quantum calculations for prevalent ion pairs (i.e., ion condensation), but the difference is not large enough to be decisive.

The model assumes that the polyelectrolyte behaves like a rigid cylinder. This cannot approximate well the behavior of a semiflexible macromolecule, in particular, the cooperatively

SCHEME 2

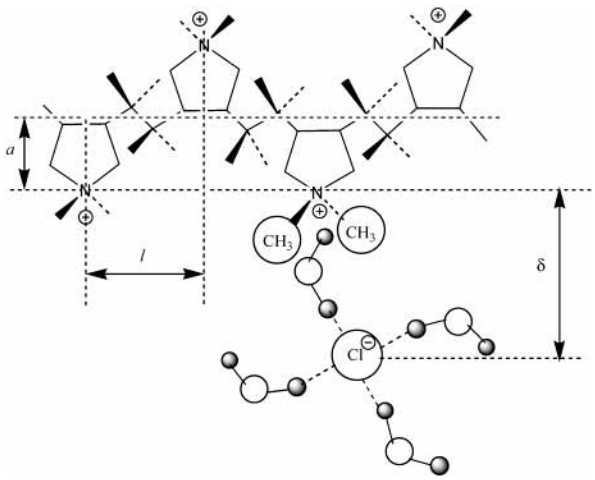

maintained local collapse. In such a *frozen fluctuation*, a definite part of counterions should be held in the vicinity of locally collapsed chain and more or less map its motions. Behavior of this kind cannot be detected by conventional relaxation but can be revealed by ^{35}Cl double-quantum spectroscopy. ΔR_2 in eq 4 happens to be equal[37−39] to the relaxation rate, R_{23}, of the second-order third-rank coherence $\mathbf{T_2^3}$, which can be measured directly by an appropriate pulse sequence:

$$R_{23} = (2\pi^2/3)[J(0) - J(2\omega_0)] \qquad (8)$$

However, there is an important difference between ΔR_2 and R_{23} given by the fact that double-quantum coherence cannot be produced unless the motion of the nucleus is either restricted (for $\mathbf{T_2^2}$) or at least hindered (for $\mathbf{T_2^3}$). According to our simulations, no double-quantum coherence can be produced for a nucleus diffusing quite freely in the sense of eq 3. However, $\mathbf{T_2^3}$ coherence spectra of PDADMAC can be detected with intensities of about 12% of the conventional $\mathbf{T_1^1}$ spectra. The corresponding relaxation rates, R_{23}, are also shown in Figure 9. The large values of R_{23} indicate that the motions of a part of the counterions correlate with those of corresponding DADMAC groups. Such behavior supports the hypothesis of cooperatively formed local collapse of the polycation chain.

As one can expect, charge screening by an added electrolyte such as NaCl promotes motion of the chain and disturbs its correlation with the counterions. As shown by Figure 11, concentrations of NaCl above 20 mmol/L drive ^{35}Cl $\mathbf{T_1^1}$ resonance to extreme narrowing ($R_1 = R_2$) and destroy the $\mathbf{T_2^3}$ coherence.

It has to be stressed that, in all of these cases, the determining mechanism of relaxation is the diffusion of the counterions from one polyion to another, differently oriented one. This is because the principal axis of the tensor of residual quadrupole coupling is aligned parallel to the local axis of the polyion chain. Consequently, diffusion along the polyion cannot relax this component and desorption leading eventually to diffusion out of the cell and encounter with another polyion with a different electric field gradient director is needed. A denser counterion condensation or even counterion−polyion correlation only leads to a stronger domination of the zero-frequency spectral density, that is, increased value of ΔR or R_{23}.

The connection of the effects already described with an electrostatic interaction between DADMAC groups can be also illustrated on the behavior of DADMAC−acrylamide copoly-

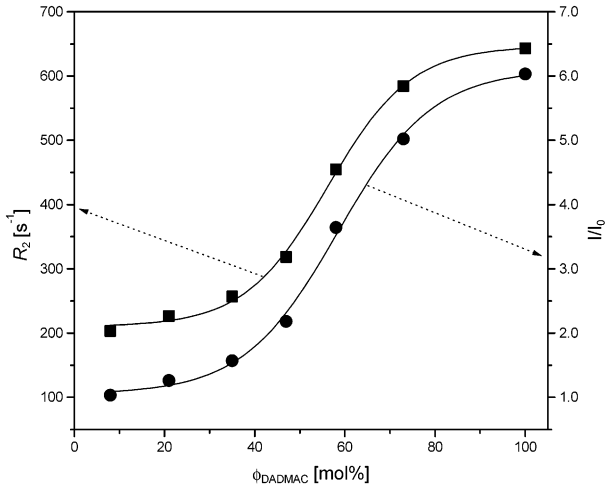

Figure 12. Dependences of the transverse (R_2) relaxation rate (monoexponential fit) of ^{35}Cl ions and maximum ^{1}H signal (1_c) intensity enhancement on the DADMAC fraction in its copolymers with acrylamide (2 mmol DADMAC/L, D_2O, 300 K)

mers with increasing DADMAC content. As shown in Figure 12, the signal intensity enhancement (signal 1_c) in ^{1}H NMR spectra between pure D_2O and 40 mmol/L NaCl is low at low contents of ionic groups in the copolymer, and such is the ^{35}Cl transverse relaxation rate (obtained by a monoexponential fit; biexponential fit is uncertain in these cases). At increased DADMAC fractions in the polymer (above 40 molar %), the probability of longer DADMAC sequences starts to be substantial and the polymer thus acquires a polyelectrolyte nature. Accordingly, we observe a marked onset of both reduction of absolute signal intensity by extreme broadening (i.e., relative intensity enhancement by ion screening) and counterion transverse relaxation rate.

Lifetime of the Local Mobility Fluctuation. The arguments contained in the previous sections support the hypothesis of a state with mobility locally promoted by cooperation between a density fluctuation of the counterions and a local chain collapse. Although stable states of such kind were predicted for relatively rigid polyelectrolytes such as DNA, they should be rather mere fluctuations in a semiflexible polymer such as PDADMAC. However, both ^{1}H transverse relaxation and ^{35}Cl quadrupolar relaxation indicate that such fluctuations should be relatively "frozen" to be detectable by NMR. It is thus of prime importance to estimate, at least in crude approximation, the average lifetime, τ_f, of such fluctuations.

Some information about the lifetime τ_f can be obtained from the inversion−recovery ^{1}H experiment. Here, the spins with $T_{2i}^* > (\gamma B_1)^{-1}$ are inverted by the first π pulse and, after some delay, d_2, their state is probed with a $\pi/2$ pulse. For sufficiently short values of d_2, we obtain a negative signal if both pulses hit the nucleus in the same coherent state. Assuming that the nuclei exchange between two sites, one of them with $T_{2j}^* < (\gamma B_1)^{-1}$ (i.e., with an extremely broad signal), such a situation cannot happen if $\tau_{ij} < d_2$ (τ_{ij} being the correlation time of exchange between states i and j). From T_1 experiments, we thus could conclude that τ_{ij} generally must be on the order of 10 ms, at least.

Another source of information about τ_{ij} is provided by the course of transverse relaxation. Let $\mathbf{M}_x$ be a column vector of the x-components of transverse magnetizations, $\mathbf{M}_x^+ \equiv (M_{x1}, M_{x2}, ... M_{xn})$ of variously mobile states 1, 2, ..., n in exchange. Following experimental data, let us assume the corresponding chemical shifts to be equal and on resonance (i.e., zero). Then the time evolution of $\mathbf{M}_x$ is described by

$$d\mathbf{M}_x/dt = \mathbf{Q}\mathbf{M}_x \tag{9}$$

where the $n \times n$ square matrix $\mathbf{Q}$ has the elements

$$Q_{jj} = -(T_{2j}^{-1} + \sum_{i \neq j} k_{ji}) \tag{10a}$$

$$Q_{ij} = k_{ij}, \qquad i \neq j \tag{10b}$$

with $k_{ij} = \tau_{ij}^{-1}$ denoting the rate constant of exchange between the states i and j. As can be shown by simulations, there are virtually three main types of relaxation decay depending on the relation between $\kappa_j = \sum_{i \neq j} k_{ji}$ and $R_{2j} = T_{2j}^{-1}$: (i) $\kappa_j \gg R_{2j}$, apparently monoexponential, with an apparent T_2 equal to a weighted mean of individual values of T_{2j}; (ii) $\kappa_j \approx R_{2j}$, approximately polyexponential, with the apparent values T_{2j}' closer to each other compared to T_{2j}; (iii) $\kappa_j \ll R_{2j}$, polyexponential, with more or less realistic values of T_{2j}. Comparison of this result with experimental data cannot distinguish between types ii and iii but excludes type i. Therefore, the lifetime of the mobile state (i.e., perturbation) must be on the order of 10 ms, at least.

Another technique, which can be used to probe exchange, is that of saturation transfer. In this experiment, a weak electromagnetic field with an intensity B_1 is placed on the signal for a time δ immediately prior to the hard $\pi/2$ pulse. Let us define the saturation ratio $\zeta_j \equiv \omega_1 T_{2j}^*$, where ω_1 is the intensity of the saturating field expressed in rad s^{-1}. If $\zeta_j < 1$, the equilibrium direct saturation of the corresponding component is incomplete, its degree being given[42,43] by ζ_j and the B_1 inhomogeneity, ΔB_1. However, saturation transfer is possible from a component with $\zeta_i > 1$ provided that there is a chemical exchange. The time development of $\mathbf{M}_z \equiv (M_{z1}, M_{z2}, ..., M_{zn})$ is generally quite analogous to eqs 9 and 10, with $\mathbf{M}_x$ and T_{2j} replaced by $\mathbf{M}_z$ and T_{1j}, respectively. In our special case, the situation is complicated by the fact that the saturating field is on-resonance for all exchanging components. In such case, the time development of I_z of the kth component is approximately (ignoring oscillatory behavior for low-saturation fields[42,43]) described by a Solomon-like equation:

$$\frac{dI_{zk}}{dt} = -R_{2\rho}^{(k)}(I_{zk} - I_{zk}^{eq}) - I_{zk}(T_{1k}^{-1} + \sum_{j \neq k} k_{kj}) + \sum_{i \neq k} k_{ik} I_{zi} \tag{11}$$

where $R_{2\rho}^{(k)} = (1/2)\xi_1 \omega_1 (T_{1k}^{-1} + T_{2k}^{-1}) + \xi_2$ (ξ_1 and ξ_2 are related to the inhomogeneity of the saturating field, $\xi_2 \approx \gamma \Delta B_1/(2\pi)$) and I_{zk}^{eq} is the equilibrium saturated intensity of the kth component under conditions of no exchange with other components, approximately given by $I_{zk}^{eq} = I_{zk}(0) \exp(-\xi_{eq}\omega_1 T_{2k})$. The spectrometer-related parameters ξ_1, ξ_2, and ξ_{eq} were calibrated by presaturation (kinetic and equilibrium) experiments performed on analogous *N*-methyl signals of a DADMAC−acrylamide copolymer containing 8 mol % of cationic groups, which has strictly monoexponential transverse relaxation and thus also simple (monoexponential) saturation behavior. In the present case, they were $\xi_1 = 2.403$, $\xi_2 = 0.081$, and $\xi_{eq} = 1.813$.

At steady state, $dI_{zk}/dt = 0$ and eq 11 turns into a set of linear equations, which can be solved for individual steady-state intensities, I_{zk}, if the values of the exchange rate constants k_{jk} (in s^{-1}) are known or, alternatively, for k_{jk}, if the intensities I_{zk} are known. In our case, we know neither of them except the starting values $I_{zk}(0) = w_k I_z(0)$ (the relative population w_k obtained by the transverse relaxation analysis reported above)

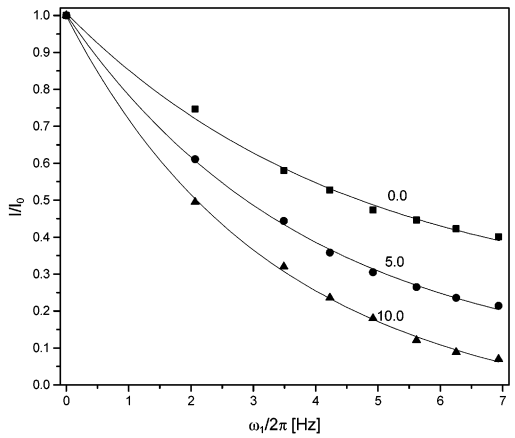

Figure 13. Experimental *N*-methyl (1t) equilibrium signal intensities at various presaturating field intensities and their best fits by eqs 11 (PDADMAC 2 mmol/L at indicated NaCl concentrations in mmol/L, 300 K).

and the cumulative steady-state intensity $I_z = \sum_k I_{zk}$ at the given saturating field intensity ω_1. We thus used the following strategy: (i) we assign the index $j = 1$ to the signal component with the highest T_{2j} (the most mobile string of DADMAC groups in the collapsed region) and generally index $j + 1$ to the component with T_{2j+1} next lower to T_{2j}; (ii) we assume that only smooth travel of the collapsed state along the chain is possible, that is, we consider only exchange between states j and $j + 1$, so that, for five components, eq 11 takes the form

$$-R_{2\rho}^{(1)}(I_{z1} - I_{z1}^{eq}) - I_{z1}({T_{11}}^{-1} + k_{1,2}) + k_{2,1}I_{z2} = 0 \quad (11a)$$

$$-R_{2\rho}^{(k)}(I_{zk} - I_{zk}^{eq}) - I_{zk}({T_{1k}}^{-1} + k_{k,k+1}) + k_{k-1,k}I_{zk-1} + k_{k+1,k}I_{zk+1} = 0, \qquad k = 2, 3, 4 \quad (11b)$$

$$-R_{2\rho}^{(5)}(I_{z5} - I_{z5}^{eq}) - I_{z5}{T_{15}}^{-1} + k_{4,5}I_{z4} = 0 \qquad (11c)$$

(iii) considering that $I_{zj}(0)$ are already equilibrium intensities, we can write (under assumption ii) $k_{j+1,j} = k_{j,j+1}w_j/w_{j+1}$ (w_j being the normalized fraction of the jth component, obtained above by transverse relaxation analysis under no saturation), reducing thus the number of optimized rate constants to one-half; (iv) assuming that chemical exchange between the components is faster than longitudinal relaxation, we take $I_{zj} = w_jI_z$; (v) as an initial guess, we take $k_{j,j+1} = {T_{1j}}^{-1}$; (vi) we optimize k_{12} to k_{45} to fit an experimental set of eight equilibrium values $I_z(\omega_1)$ for increasing ω_1.

Figure 13 shows the experimental points for 2 mmol/L DADMAC in D_2O containing 0.0, 5.0, and 10.0 mmol NaCl/L and the best fits. The optimal values of k_{12} to k_{45} are given in Table 1. Individual lifetimes, τ_k, of the components were calculated according to the formula $\tau_k = (1/2)({k_{k,k+1}}^{-1} + {k_{k+1,k}}^{-1})$, whereas the mean lifetime of the fluctuation is $\tau_f = \sum_k w_k\tau_k$. As it can be seen, the values of τ_k are comparable with T_{2k}, though usually several times larger. Multiexponential transverse decay of the signal is thus possible, but the apparent values of T_{2k} are nearer to each other than the real ones. In other words, the differences in mobility are even larger than suggested by the transverse relaxation analysis. The τ_f values are generally larger than those estimated above as lower bounds, which adds to the general credibility of the analysis.

The obtained τ_f values cannot be precise because of the rather gross approximations used in their estimation, but they should be at least correct in their order of magnitude. As such, they

TABLE 1: Optimized Values of w_i, T_{1i}, T_{2i}, $k_{i,i+1}$, and τ_i for the Components of the PDADMAC 1_c Signal in Media of Different Ionic Strengths

C_{NaCl}, mmol/L	i	w_i	T_1, s	T_{2i}, ms	$k_{i,i+1}$, s^{-1}	τ_i, s	τ_f, s
0.0	1	0.07	0.267	31.1	16.3	0.096	0.065
	2	0.15		19.2	15.8	0.084	
	3	0.25		9.5	18.4	0.059	
	4	0.29		5.0	17.7	0.052	
	5	0.24		1.6			
5.0	1	0.14	0.323	31.5	17.9	0.066	0.056
	2	0.19		19.3	18.3	0.068	
	3	0.28		11.4	16.7	0.054	
	4	0.25		6.0	18.8	0.042	
	5	0.14		2.4			
10.0	1	0.34	0.341	31.5	19.9	0.050	0.043
	2	0.33		24.5	18.8	0.045	
	3	0.23		11.6	18.9	0.036	
	4	0.08		6.2	20.2	0.034	
	5	0.02		2.5			

are surprisingly large, if the observed mobile state is considered as a liquid-state fluctuation. In agreement with the ^{35}Cl quadrupolar-relaxation analysis, we should consider the fluctuation as relatively "frozen" or stabilized by a cooperative interaction of the locally collapsed chain with the surrounding chloride counterions.

Conclusions

We have shown that the chains of a DADMAC polymer in its dilute water solution and under conditions of low ionic strength, that is, low concentrations of the polyelectrolyte and additional salt, exhibit transient regions of increased local conformation mobility. According to absolute signal intensity in ^1H NMR, the size of the mobile regions increases with increasing ionic strength brought about by higher polymer concentration or by addition of a low-molecular-weight electrolyte to the solution or both. It also decreases with increasing molecular weight of DADMAC polymer, but the convergent shape of the dependence above 2×10^5 excludes the possibility that the higher mobility regions correspond to chain ends only.

Signal intensity changes in ^1H NMR are brought about by a changing fraction of DADMAC groups giving rise to extremely broadened NMR signals. Because the actual absolute intensity is as low as $1/6$ of the theoretical value, such groups are in majority under low ionic strength. Double-quantum ^1H NMR signals of *N*-methyl protons verify that broadening of NMR signals is due to a hindered local conformation change of the polymer backbone, giving rise to motional anisotropy relative to the NMR time window. As shown by ^1H NMR transverse relaxation analysis, the DADMAC groups, which are mobile enough to offer visible signals, form regions with a broad local mobility distribution. Ionic strength, increased either by added electrolyte or by increased polymer concentration, increases both the size of such regions and the relative population of groups with higher mobility in them.

The absence or weak expression of such effects in DADMAC−acrylamide copolymers with low contents of ionic groups and their gradual onset with increasing DADMAC fraction in the polymer (above 40 molar %) show that they are due to the interactions of neighboring DADMAC groups. The strong dependence of the effects on ionic screening due to increased ionic strength shows that these interactions are of an electrostatic nature. Simulations by quantum-mechanical calculations predict strong dependence both of the chain conformation and of the barrier to its change on the ionization state of the DADMAC groups, stressing thus the importance of counterion density

SCHEME 3

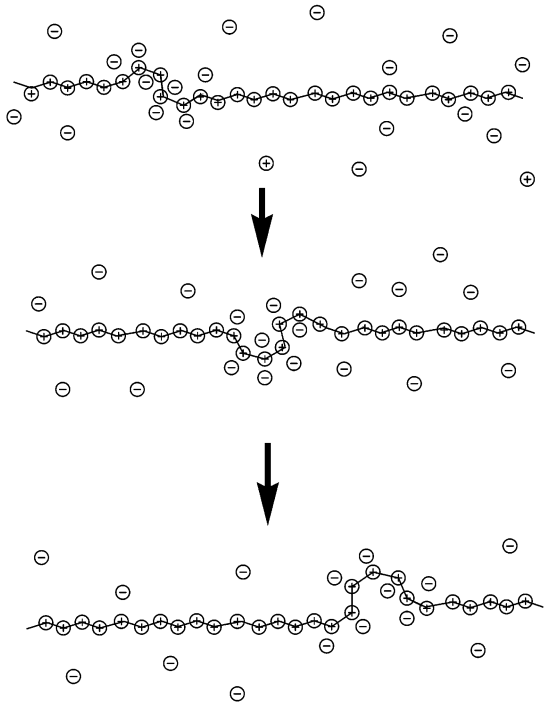

fluctuations. Probing the behavior of chloride counterions by ^{35}Cl NMR quadrupolar relaxation gives a reasonable agreement of experimental concentration dependence of its longitudinal and transverse relaxation rates with predictions of combined Poisson−Boltzmann and Smoluchowski equations. However, the rate and extent of double-quantum quadrupolar relaxation at varying ionic strength show that the dynamics of a fraction of counterions defies the requirements of a mean-field-determined diffusion statistics and correlates with the motions of the polymer. These effects arise precisely at conditions also giving rise to large fluctuations in local chain mobility. This leads to a plausible conclusion that the perturbation of chain behavior leading to increased local mobility is connected with locally increased counterion condensation. Because of screening by the counterions, intrachain electrostatic repulsions are weakened in the perturbed area, which leads to a less-extended chain. Therefore, we call the fluctuation local chain collapse.

Chain collapse due to counterion density fluctuation has been theoretically predicted for stiff polyelectrolytes such as DNA. In flexible or semiflexible polyelectrolytes such as PDADMAC, it could be expected to occur in a form of only transient local fluctuation. However, estimation by three independent methods (inversion−recovery, transverse relaxation, and in particular, saturation transfer experiments) puts its average lifetime into the range between 30 and 80 ms. The fluctuation thus appears to be relatively "frozen", that is, stabilized by a cooperative behavior of counterions and the polyion chain. Mutual exchange between the sites with different local mobility, detected by saturation transfer experiments, indicates that the fluctuation does not necessarily expire by total disintegration but more probably travels to-and-fro (cf. Scheme 3) along the chain.

At the very end, we would like to stress that the cooperative fluctuation described here is not analogous but rather complementary to the well-known hypercoiling[44] of some polymers such as DNA or poly(methacrylic acid). In both phenomena, the area of different mobility is formed by frozen fluctuation of the polymer ionization. However, such fluctuation leads to a state with locally hindered motion in hypercoiling but to a state with promoted local mobility in our case of local chain collapse.

Acknowledgment. The authors thank the Grand Agency of Academy of the Czech Republic for financial support of this study given under Grants A4050206 and K4050111. They also thank Dr. H. Dautzenberg from the Max-Planck-Institute for Colloid and Interface Research, Berlin, for samples of DADMAC polymer and Prof. Y. Levin from the University of Rio Grande do Sul, Brazil, for discussion of the problems of counterion distribution. Thanks are also due to Mrs. D. Kaňková for technical assistance.

References and Notes

(1) Oozawa, F. *Polyelectrolytes*; M. Dekker: New York, 1971.
(2) Dautzenberg, H.; Jaeger, W.; Kötz, J,; Philip, B.; Seidel, Ch.; Stscherbina, D. *Polyelectrolytes*; Hanser Publishers: Munich, Germany, 1994.
(3) Förster, S.; Schmidt, M. *Adv. Polymer Sci.* **1995**, *120*, 51.
(4) Barrat, J.-L.; Joanny, J.-F. *Adv. Chem. Phys.* **1995**, *94*, 1.
(5) Dobrynin, A. V.; Rubinstein, M.; Obukhov, S. P. *Macromolecules* **1996**, *29*, 2974.
(6) Liverpool, T. B.; Stapper, M. *Europhys. Lett.* **1997**, *40*, 485.
(7) Muthukumar, M. *J. Chem. Phys.* **1997**, *107*, 2619.
(8) Brilliantov, N. V.; Kuznetsov, D. V.; Klein, R. *Phys. Rev. Lett.* **1998**, *81*, 1433.
(9) Golestanian, R.; Kardar, M.; Liverpool, T. B. *Phys. Rev. Lett.* **1999**, *82*, 4456.
(10) Deshkovski, A.; Obukhov, S.; Rubinstein, M. *Phys. Rev. Lett.* **2001**, *86*, 2341.
(11) Micka, U.; Kremer, K. *Phys. Rev.* **1996**, *E54*, 2653. Micka, U.; Kremer, K. *J. Phys.: Condens. Matter* **1996**, *8*, 9463. Micka, U.; Kremer, K. *Europhys. Lett.* **1997**, *38*, 279.
(12) Stevens, M.; Kremer, K. *J. Chem. Phys.* **1995**, *103*, 1669. Stevens, M.; Kremer, K. *Phys. Rev. Lett.* **1993**, *71*, 2228. Stevens, M.; Kremer, K. *Macromolecules* **1993**, *26*, 4717.
(13) Deserno, M.; Holm, C. *J. Chem. Phys.* **1998**, *109*, 7678, 7694.
(14) Holm, C.; Kremer, K. In *Proceedings of the Yamada Conference "Polyelectrolytes"*; Noda, I., Kokufuta, E., Eds.; Inuyama, 2000, p 27.
(15) Stevens, M. J.; Plimpton, S. J. *Eur. Phys. J.* **1998**, *B2*, 341.
(16) Chu, J. C.; Mak, C. H. *arXiv: cond-mat/9811204v1*.
(17) Deserno, M.; Holm, C.; May, S. *Macromolecules* **2000**, *33*, 199.
(18) Limbach, H. J.; Holm, C. *J. Chem Phys.* **2001**, *114*, 9674.
(19) Odijk, T. *J. Polym. Sci., Part B: Polym. Phys.* **1977**, *15*, 477. Odijk, T. *Polymer* **1978**, *19*, 989. Skolnick, J.; Fixman, M. *Macromolecules* **1977**, *10*, 944. Fixman, M. *J. Chem. Phys.* **1982**, *76*, 6242. Tricot, M. *Macromolecules* **1984**, *17*, 1698. Ha, B.-Y.; Thirumalai, D. *Macromolecules* **1995**, *28*, 577.
(20) Foerster, S.; Schmidt, M.; Antonietti, M. *Polymer* **1990**, *31*, 781.
(21) Smits, R. G.; Kuil, M. E.; Mandel, M. *Macromolecules* **1993**, *26*, 6808. Tanahatoe, J. J.; Kuil, M. E. *Macromolecules* **1997**, *30*, 6102. Tanahatoe, J. J.; Kuil, M. E. *J. Phys. Chem. B* **1997**, *101*, 10839. Sedlak, M. *J. Chem. Phys.* **1996**, *105*, 10123. Borochov, N.; Eisenberg, H. *Macromolecules* **1994**, *27*, 1440.
(22) Tanahatoe, J. J. *J. Phys. Chem. B* **1997**, *101*, 10442.
(23) Schipper, F. J. M.; Leyte, J. C. *J. Phys.: Condens. Matter* **1997**, *9*, 11179.
(24) Kříž, J.; Masaø, M.; Dybal, J.; Doskoèilová, D. *Macromolecules* **1997**, *30*, 3302.
(25) Lindman, B. In *NMR of Newly Accessible Nuclei*; Laszlo, P., Ed.; Academic Press: New York, 1983; Vol. 1, p 193.
(26) Halle, B.; Wennerström, H.; Piculell, L. *J. Phys. Chem.* **1984**, *88*, 2482.
(27) Halle, B.; Bratko, D.; Piculell, L. *Ber. Bunsen-Ges. Phys. Chem.* **1985**, *89*, 1254.
(28) Schipper, F. J. M.; Hollander, J. G.; Leyte, J. C. *J. Phys.: Condens. Matter* **1997**, *9*, 11179; **1998**, *10*, 9207.
(29) Brand, F.; Dautzenberg, H.; Jaeger, W.; Hahn, M. *Angew. Makromol. Chem.* **1997**, *248*, 41. Brand, F.; Dautzenberg, H. *Langmuir* **1997**, *13*, 2905. Dautzenberg, H. *Macromolecules* **1997**, *30*, 7810.
(30) Kříž, J.; Dautzenberg, H. *J. Phys. Chem. A* **2001**, *105*, 3846. Kříž, J.; Dybal, J.; Dautzenberg, H. *J. Phys. Chem. A* **2001**, *105*, 7486. Kříž, J.; Dybal, J.; D. Kurková *J. Phys. Chem. A*, in press.
(31) Kříž, J.; Kurková, D.; Dybal, J.; Oupický, D *J. Phys. Chem. A* **2000**, *104*, 10972.
(32) Kay, L. E.; Prestergard, J. H. *J. Am. Chem. Soc.* **1987**, *109*, 3829.

(33) Wong, T. C.; Wang, P.-L.; Duh, D.-M.; Hwang, L.-P. *J. Phys. Chem.* **1989**, *93*, 1295.
(34) Tanner, J. E. *J. Chem. Phys.* **1970**, *52*, 2523. Cotts, R. M.; Hoch, M. J. R.; Sun, T.; Markert, J. T. *J. Magn. Reson.* **1989**, *83*, 252.
(35) Hertz, H. G.; Holz, M. *J. Phys. Chem.* **1974**, *78*, 1002.
(36) Bull, T. E. *J. Magn. Reson.* **1972**, *8*, 344.
(37) Jung, K. J.; Tauskela, J. S.; Katz, J. *J. Magn. Reson. B* **1996**, *112*, 103.
(38) Eliav, U.; Navon, G. *J. Magn. Reson. A* **1996**, *123*, 32.
(39) Jung, K. J.; Katz, J. *J. Magn. Reson. B* **1996**, *112*, 214.
(40) Kříž, J.; Brus, J.; Pleštil, J.; Kurková, D.; Masař, B.; Dybal, J.; Zune, C.; Jerôme, R. *Macromolecules* **2000**, *33*, 4108−4115.
(41) Hertz, H. G.; Holz, M. *J. Phys. Chem.* **1974**, *78*, 1002.
(42) Neuhaus, D.; Williamson, M. P. *The Nuclear Overhauser Effect in Structural and Conformational Analysis*; VCH Publishers: New York, Weinheim, Germany, Cambridge, U.K., 1989; p 145.
(43) Dobson, C. M.; Olejniczak, E. T.; Poulsen, F. M.; Ratcliffe, R. G. *J. Magn. Reson.* **1982**, *48*, 97.
(44) Dubin, P. L.; Strauss, U. P. In *Polyelectrolytes and their applications*; Rembaum, A., Sélégny, E., Eds.; Reidel: New York, 1975.